

A Novel Single-Loop Decoupled Schoenflies-Motion Generator: Concept and Kinematics Analysis

Raffaele Di Gregorio^(✉)

Department of Engineering, University of Ferrara, Ferrara, Italy
raffaele.digregorio@unife.it

Abstract. Schoenflies-motion generators (SMGs) are 4-degrees-of-freedom (dof) manipulators whose end effector can perform translations along three independent directions and rotations around one fixed direction (Schoenflies motions). Such motions constitute the 4-dimensional (4-D) Schoenflies subgroup of the 6-D displacement group. The most known SMGs are the serial robots named SCARA. Pick-and-place tasks are typical industrial applications that can be accomplished by SMGs. Over the SCARA, lower-mobility parallel manipulators (PMs) have been proposed as SMGs. Here, a novel type of SMG with parallel architecture is presented together with its kinematics analysis. The proposed SMG has a single-loop not-overconstrained architecture, actuators on or near the base and decoupled kinematics.

Keywords: Parallel manipulators · Schoenflies subgroup · Position analysis · Singularity analysis · Decoupled kinematics

1 Introduction

A number of industrial applications (e.g., pick-and-place tasks) require rigid body's translations along three independent directions together with rotations around one fixed direction. The displacement set of this type constitutes the 4-D Schoenflies subgroup of the 6-D displacement group [1–3] and the 4-dof manipulators whose end effector is constrained to perform Schoenflies displacements are called Schoenflies-motion generators (SMGs) [2]. The most known SMGs are the serial robots named SCARA.

Parallel SMGs have been also proposed in the literature (see, for instance, [3–11]). Parallel architectures feature two rigid bodies, one fixed (base) and the other movable (platform), that are connected with one another by a number of kinematic chains (limbs). Most of the parallel SMGs have four limbs (e.g., [4–6, 8, 11]) and one actuator per limb located on the base. Nevertheless, two-limbed symmetric (i.e., single-loop) architectures with serial [3] or hybrid [7, 10] limbs have been proposed, too. Other parallel SMG are simply obtained by adding a double Cardan shaft (i.e., a limb of RUPUR¹ type), which connects the base to the platform, in a translational parallel manipulator.

¹ Hereafter, R, P, U, S, and C stand for revolute pair, prismatic pair, universal joint, spherical pair, and cylindrical pair respectively. The underlining indicates the actuated joints and the sequence of joint types, which are encountered by moving from the base to the platform on a limb, is given with a string of capital letters.

Parallel SMGs are faster [6] than their serial counterparts due to the possibility, they have, of locating the actuators on the base. Nevertheless, reduced workspace and cumbersome multi-loop topologies with complex kinematics are their main drawbacks. In particular, parallel SMGs usually cannot make the platform perform a complete rotation and some tricks have to be devised to overcome this drawback [12]. So, reducing the limb number by keeping the actuators on or near the base is an appealing design choice. This can be done by adopting single-loop architectures with two actuators per limb [3].

Also, the possibility of decoupling position and orientation (decoupled kinematics) would allow simpler and more intuitive control strategies, and a not-overconstrained architecture would make it possible to avoid jamming without using small tolerances during manufacturing. Here, a novel parallel SMG of PRRS-RRC type (Fig. 1) is presented together with its kinematics analysis. The proposed SMG has a single-loop not-overconstrained architecture, actuators on or near the base and a simple and decoupled kinematics.

The paper is organized as follows. Section 2 presents the novel SMG. Then, Sect. 3 solves in closed form its direct and inverse position analyses. Eventually, Sect. 4 discusses the most critical issues of the proposed SMG, and Sect. 5 draws the conclusions.

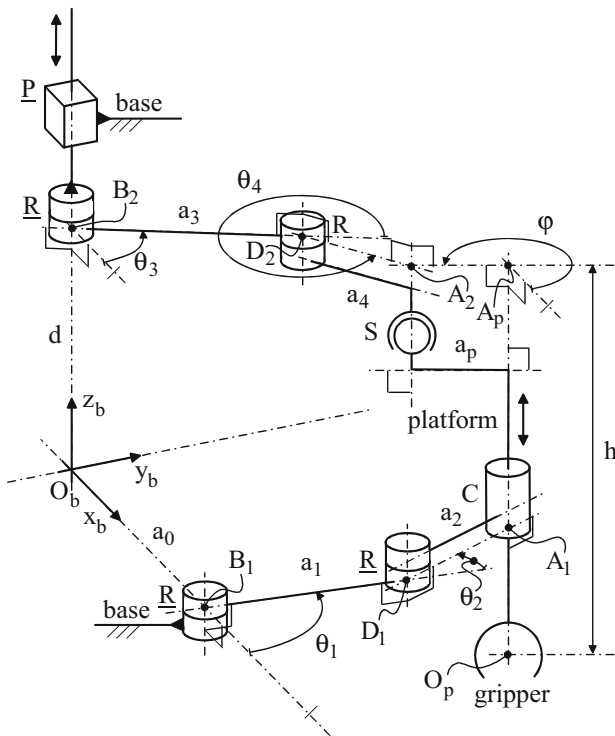


Fig. 1. The PRRS-RRC Schoenflies-motion generator

2 The PRRS-RRC Schoenflies-Motion Generator

Figure 1 shows the SMG of PRRS-RRC type. With reference to Fig. 1, the platform is connected to the base by two limbs, one of PRRS type and the other of RRC type, which form a single-loop not-overconstrained spatial mechanism with 4 dof. The Cartesian reference $O_b x_b y_b z_b$ is fixed to base. The axes of the R and C pairs and the sliding direction of the P pair are all parallel to the z_b axis.

In the PRRS limb (see Fig. 1), the P pair and the adjacent R pair are actuated. Point B_2 lies on the axis of the actuated R pair and is fixed to the slider of the P pair. The actuated-joint variable of the P pair is the signed distance, d , of B_2 from O_b . The plane parallel to the $x_b y_b$ plane and passing through B_2 intersects the axis of the passive R pair at D_2 , the axis of the C pair at A_p , and the axis parallel to the z_b axis and passing through the center of the S pair at A_2 . a_3 and a_4 are the lengths of the segments $B_2 D_2$ and $D_2 A_2$, respectively; whereas, θ_3 and θ_4 are the joint variables of the actuated R pair and of the passive R pair, respectively. The point A_p is fixed to the platform.

In the RRC limb (see Fig. 1), the two R pairs are actuated. Their actuated-joint variables are θ_1 and θ_2 . The $x_b y_b$ plane intersects the axis of the R pair adjacent to the base at B_1 , the axis of the other R pair at D_1 , and the axis of the C pair at A_1 . a_0 , a_1 and a_2 are the lengths of the segments $O_b B_1$, $B_1 D_1$ and $D_1 A_1$, respectively.

Regarding the platform (see Fig. 1), a_p is the constant distance of the center of the S pair from the axis of the C pair and is equal to the length of the segment $A_p A_2$. O_p is the reference point of the platform, and h is the length of the segment $A_p O_p$.

Hereafter, the coordinates of O_p measured in $O_b x_b y_b z_b$ will be denoted $(x_p, y_p, z_p)^T$ and will locate the position of the platform; whereas, the angle, φ , between the segment $A_p A_2$ and a line parallel to x_b and passing through A_p (see Fig. 1) will be used to uniquely determine the platform orientation.

The RRC limb constrains the platform to perform Schoenflies motions with rotation axis parallel to the z_b axis. As it will be clearer later, it controls the position of point A_1 on the $x_b y_b$ plane through its two actuated R pairs; whereas, the PRRS limb controls the coordinate z_p of point O_p through the actuated P pair and, independently, the platform orientation through its actuated R pair.

3 Position Analysis

According to the above-introduced notations, the 4-tuple $\mathbf{q} = (\theta_1, \theta_2, \theta_3, d)^T$ collects the coordinates of the joint space (i.e., all the actuated-joint variables); whereas, the 4-tuple $\mathbf{\kappa} = (x_p, y_p, z_p, \varphi)^T$ collects the coordinates of the operational space that uniquely define the platform pose.

The analysis of the RRC limb (Fig. 1) brings to write the following relationships

$$x_p = a_0 + a_1 \cos \theta_1 + a_2 \cos(\theta_1 + \theta_2) \quad (1a)$$

$$y_p = a_0 + a_1 \sin \theta_1 + a_2 \sin(\theta_1 + \theta_2) \quad (1b)$$

Moreover, the analysis of the PRRS limb yields

$$x_p = a_3 \cos \theta_3 + a_4 \cos(\theta_3 + \theta_4) - a_p \cos \varphi \quad (2a)$$

$$y_p = a_3 \sin \theta_3 + a_4 \sin(\theta_3 + \theta_4) - a_p \sin \varphi \quad (2b)$$

$$z_p = d - h \quad (2c)$$

3.1 Direct Position Analysis

The direct position analysis (DPA) consists in calculating the platform poses (i.e., the values of κ) compatible with assigned values of the actuated-joint variables (i.e., with one value of \mathbf{q}). The closed-form solution of the DPA follows.

Since, in the DPA, the values of θ_1 , θ_2 and d are assigned, Eqs. (1a), (1b), and (2c) straightforwardly give a unique value for x_p , y_p , and z_p (i.e., for the platform position), respectively. Once x_p and y_p have been computed, the elimination of $\cos(\theta_3 + \theta_4)$ and $\sin(\theta_3 + \theta_4)$ from Eqs. (2a) and (2b), obtained by exploiting the trigonometric identity $\cos^2 x + \sin^2 x = 1$, yields

$$(x_p + a_p \cos \varphi - a_3 \cos \theta_3)^2 + (y_p + a_p \sin \varphi - a_3 \sin \theta_3)^2 = a_4^2 \quad (3)$$

which can be transformed as follows by expanding and simplifying its left-hand side

$$b_0 + b_1 \sin \varphi + b_2 \cos \varphi = 0 \quad (4)$$

where $b_0 = x_p^2 + y_p^2 + a_p^2 + a_3^2 - a_4^2 - 2a_3(x_p \cos \theta_3 + y_p \sin \theta_3)$, $b_1 = 2a_p(y_p - a_3 \sin \theta_3)$, and $b_2 = 2a_p(x_p - a_3 \cos \theta_3)$. Since, in the DPA, θ_3 is known, Eq. (4) is a trigonometric equation that contains only one unknown: the angle φ . The introduction of the trigonometric identities $\cos \varphi = (1 - t^2) / (1 + t^2)$ and $\sin \varphi = 2t / (1 + t^2)$ with $t = \tan(\varphi / 2)$ into Eq. (4) yields the following quadratic equation

$$t^2(b_0 - b_2) + 2t b_1 + (b_0 + b_2) = 0 \quad (5)$$

whose two solutions are

$$\varphi_{1,2} = 2 \arctan \left(\frac{-b_1 \pm \sqrt{b_1^2 + b_2^2 - b_0^2}}{b_0 - b_2} \right) \quad (6)$$

The two values of φ (i.e., the two platform orientations), Eq. (6) provides, depend only on the assigned value of the actuated-joint variable θ_3 . From a geometric point of view, they correspond to the two intersections of the two circumferences, one with center at D_2 and radius a_4 and the other with center at A_p and radius a_p , that lie on the plane parallel to the $x_b y_b$ plane and passing through B_2 .

The conclusions are: (i) the DPA can be solved by using simple explicit formulas, and (ii) the DPA has one solution for the platform position that depends only on the actuated-joint variables θ_1 , θ_2 and d and two solutions for the platform orientation that depend only on the remaining actuated-joint variable θ_3 (i.e., position and orientation are decoupled).

3.2 Inverse Position Analysis

The inverse position analysis (IPA) consists in calculating the actuated-joint variables (i.e., the values of \mathbf{q}) compatible with an assigned platform pose (i.e., with one value of $\mathbf{\kappa}$). The closed-form solution of the IPA follows.

Since, in the IPA, the values of x_p , y_p , and z_p are assigned, the actuated-joint variable d can be immediately computed from Eq. (2c) as follows: $d = z_p + h$; whereas, θ_1 and θ_2 can be computed by solving the system of two equations in two unknowns constituted by Eqs. (1a) and (1b). Indeed, the elimination of $\cos(\theta_1 + \theta_2)$ and $\sin(\theta_1 + \theta_2)$ from Eqs. (1a) and (1b), obtained by exploiting the trigonometric identity $\cos^2 x + \sin^2 x = 1$, yields

$$(x_p - a_0 - a_1 \cos \theta_1)^2 + (y_p - a_0 - a_1 \sin \theta_1)^2 = a_2^2 \quad (7)$$

which can be transformed as follows by expanding and simplifying its left-hand side

$$c_0 + c_1 \sin \theta_1 + c_2 \cos \theta_1 = 0 \quad (8)$$

where $c_0 = (x_p - a_0)^2 + (y_p - a_0)^2 + a_1^2 - a_2^2$, $c_1 = -2a_1(y_p - a_0)$, and $c_2 = -2a_1(x_p - a_0)$.

Then, the introduction of the trigonometric identities $\cos \theta_1 = (1 - f^2) / (1 + f^2)$ and $\sin \theta_1 = 2f / (1 + f^2)$ with $t = \tan(\theta_1 / 2)$ into Eq. (8) yields the following quadratic equation

$$f^2(c_0 - c_2) + 2f c_1 + (c_0 + c_2) = 0 \quad (9)$$

whose two solutions are

$$(\theta_1)_{1,2} = 2 \arctan \left(\frac{-c_1 \pm \sqrt{c_1^2 + c_2^2 - c_0^2}}{c_0 - c_2} \right) \quad (10)$$

Once, the two values of θ_1 have been computed through formula (10) the two corresponding values of θ_2 can be computed from Eqs. (1a) and (1b) as follows:

$$\theta_2 = \text{ATAN2}[(y_p - a_0 - a_1 \sin \theta_1), (x_p - a_0 - a_1 \cos \theta_1)] - \theta_1 \quad (11)$$

From a geometric point of view, the two computed solutions of (θ_1, θ_2) correspond to the two intersections of the two circumferences of the $x_b y_b$ plane one with center at A_1 and radius a_2 and the other with center at B_1 and radius a_2 .

Eventually, since the angle φ is assigned in the IPA, Eq. (3) has the only unknown θ_3 . Such equation can be transformed as follows by expanding and simplifying its left-hand side

$$g_0 + g_1 \sin \theta_3 + g_2 \cos \theta_3 = 0 \quad (12)$$

where $g_0 = (x_p + a_p \cos \varphi)^2 + (y_p + a_p \sin \varphi)^2 + a_3^2 - a_4^2$, $g_1 = -2a_3(y_p + a_p \sin \varphi)$, and $g_2 = -2a_3(x_p + a_p \cos \varphi)$. After the introduction of the trigonometric identities $\cos \theta_3 = (1 - s^2) / (1 + s^2)$ and $\sin \theta_3 = 2s / (1 + s^2)$ with $s = \tan(\theta_3/2)$, Eq. (12) becomes the following quadratic equation in s

$$s^2(g_0 - g_2) + 2s g_1 + (g_0 + g_2) = 0 \quad (13)$$

whose two solutions are

$$(\theta_3)_{1,2} = 2 \arctan \left(\frac{-g_1 \pm \sqrt{g_1^2 + g_2^2 - g_0^2}}{g_0 - g_2} \right) \quad (14)$$

From a geometric point of view, the two values of θ_3 computed with formula (14) correspond to the two intersections of the two circumferences, one with center at A_2 and radius a_4 and the other with center at B_2 and radius a_3 , that lie on the plane parallel to the $x_b y_b$ plane and passing through B_2 .

The conclusion is that the IPA has only one solution for d and, at most, four solutions for $(\theta_1, \theta_2, \theta_3)$, that is, at most four values of \mathbf{q} are compatible with one value of $\mathbf{\kappa}$.

4 Discussion

The singularity analysis is a central issue for parallel mechanisms. Singularities are mechanism configurations where the linear relationship between actuated-joint rates and platform twist (instantaneous input-output relationship (InI/O)) fails. In the studied SMG, configurations (constraint singularities) where the platform instantaneous motion may not be a Schoenflies motion are not present since the RRC limb has always connectivity four. The absence of constraint singularities makes it possible to deduce the InI/O by taking into account only $\dot{\mathbf{\kappa}} = (\dot{x}_p, \dot{y}_p, \dot{z}_p, \dot{\phi})^T$, instead of the whole platform twist, as instantaneous output. The time derivatives of Eqs. (1a), (1b), (2c), and (3) yield the following InI/O

$$\dot{x}_p = -[a_1 \sin \theta_1 + a_2 \sin(\theta_1 + \theta_2)]\dot{\theta}_1 - a_2 \sin(\theta_1 + \theta_2)\dot{\theta}_2 \quad (15a)$$

$$\dot{y}_p = [a_1 \cos \theta_1 + a_2 \cos(\theta_1 + \theta_2)]\dot{\theta}_1 + a_2 \cos(\theta_1 + \theta_2)\dot{\theta}_2 \quad (15b)$$

$$\dot{z}_p = \dot{d} \quad (15c)$$

$$m_x \dot{x}_p + m_y \dot{y}_p + \dot{\phi} a_p (m_y \cos \phi - m_x \sin \phi) = \dot{\theta}_3 a_3 (m_y \cos \theta_3 - m_x \sin \theta_3) \quad (15d)$$

where $m_x = x_p + a_p \cos \phi - a_3 \cos \theta_3$ and $m_y = y_p + a_p \sin \phi - a_3 \sin \theta_3$.

The analysis of Eqs. (15a)–(15d) reveals that, if the actuated-joint rates are assigned, $\dot{\mathbf{O}}_p = (\dot{x}_p, \dot{y}_p, \dot{z}_p)^T$ is always uniquely determined, but $\dot{\phi}$ is not determined when the segments A_2D_2 and A_2A_p are aligned (i.e., a parallel singularity occurs). Also, it reveals that, if \mathbf{k} is assigned, only two geometric conditions make one or more actuated-joint rates undetermined (i.e., a serial singularity² occurs): (i) the 2-tuple $(\dot{\theta}_1, \dot{\theta}_2)$ is not determined when the segments A_1D_1 and D_1B_1 are aligned, and (ii) $\dot{\theta}_3$ is not determined when the segments A_2D_2 and D_2B_2 are aligned.

If the actuated P pair and the two actuated R pairs of the RRC limb are locked, the position of point A_p (Fig. 1) will be locked, too, and the segments B_2A_p , B_2D_2 , D_2A_2 , and A_pA_2 will behave like frame, input link, coupler, and follower, respectively, of a four-bar linkage with θ_3 and ϕ as input and output variables, respectively. The singularities of this four-bar linkage correspond to the above-identified parallel singularity and serial singularity (ii). Also, if Grashof's rule is satisfied and A_pA_2 is the shortest bar the angle ϕ can perform a complete rotation. In general, the angle ϕ can always perform a complete rotation if and only if $(a_3 + a_4) \geq (a_p + \sqrt{x_p^2 + y_p^2})$. Unfortunately, the parallel singularity condition is encountered two times during a complete rotation of the platform. Nevertheless, this parallel singularity can be safely crossed by suitably changing the length and/or the orientation of the frame B_2A_p with the RRC limb.

Eventually, it is worth stressing that two coaxial motors put on the base can drive both the two actuated R pairs of the RRC limb since a toothed belt can transmit the motion to the second R pair. So, the proposed SMG practically has three actuators on the base and only one near the base.

5 Conclusions

A novel parallel Schoenflies-motion generator of PRRS-RRC type has been presented together with its kinematics analysis. The proposed PRRS-RRC has a single-loop not-overconstrained architecture, actuators on or near the base and a simple and decoupled kinematics.

In particular, both the direct and the inverse position analyses are solved by using simple explicit formulas with a clear geometric meaning. Three actuators control the platform position and, independently, the remaining fourth controls the platform rotation. There is no constraint singularity, and only one parallel singularity condition safely crossable by using suitable path planning strategies for making the platform perform a complete rotation.

² It is worth reminding that serial singularities lie on (and identify) the workspace boundary.

Future works will address the dimensional synthesis and the dynamic behavior of the proposed manipulator.

Acknowledgments. This work has been developed at the Laboratory of Advanced Mechanics (MECH-LAV) of Ferrara Technopole, supported by FIR2016 funds and by Regione Emilia Romagna (District Councillorship for Productive Assets, Economic Development, Telematic Plan) POR-FESR 2007-2013€, Attività I.1.1

References

1. Hervé JM (1999) The Lie group of rigid body displacements, a fundamental tool for mechanism design. *Mech Mach Theor* 34:719–730
2. Lee C-C, Hervé JM (2009) Type synthesis of primitive schoenflies-motion generators. *Mech Mach Theor* 44:1980–1997
3. Lee C-C, Hervé JM (2011) Isoconstrained parallel generators of schoenflies motion. *ASME J Mech Rob* 3:021006
4. Pierrot F, Company O (1999) H4: a new family of 4-DOF parallel robots. In: *IEEE/ASME International Conference on Advanced Intelligent Mechatronics (AIM 1999)*, Atlanta, Georgia, USA, pp 508–513
5. Krut S, Company O, Benoit M, Ota H, Pierrot F (2003) I4: a new parallel mechanism for SCARA motions. In: *Proceedings of 2003 International Conference on Robotics and Automation*, Taipei, Taiwan, pp 1875–1880
6. Nabat V, de la O Rodriguez M, Company O, Krut S, Pierrot F (2005) Par4: very high speed parallel robot for pick-and-place. In: *Proceedings of 2005 IEEE/RSJ International Conference on Intelligent Robots and Systems*, pp 553–558
7. Angeles J, Caro S, Khan W, Morozov A (2006) The design and prototyping of an innovative schoenflies motion generator. *Proc IMechE-Part C J Mech Eng* 220(C7):935–944
8. Li Z, Lou Y, Zhang Y, Liao B, Li Z (2013) Type synthesis, kinematic analysis, and optimal design of a novel class of schoenflies-motion parallel manipulators. *IEEE Trans Aut Sc Eng* 10:674–686
9. Kong X, Gosselin CM (2004) Type synthesis of 3T1R 4-DOF parallel manipulators based on screw theory. *IEEE Trans Rob Autom* 20:181–190
10. Company O, Pierrot F, Nabat V, Rodriguez M (2005) Schoenflies motion generator: a new non redundant parallel manipulator with unlimited rotation capability. In: *Proceedings of 2005 IEEE International Conference on Robotics and Automation*, Barcelona, Spain, pp 3250–3255
11. Richard P-L, Gosselin CM, Kong X (2007) Kinematic analysis and prototyping of a partially decoupled 4-DOF 3T1R parallel manipulator. *ASME J Mech Des* 129:611–616
12. Pierrot F, Company O, Krut S, Nabat V (2006) Four-DOF PKM with articulated travelling-plate. In: *PKS 2006: Parallel Kinematics Seminar*, Chemnitz, Germany, pp 25–26. <lirmm-00105558>

Advances in Service and Industrial Robotics
Proceedings of the 26th International Conference on
Robotics in Alpe-Adria-Danube Region, RAAD 2017
Ferraresi, C.; Quaglia, G. (Eds.)
2018, XIX, 1047 p. 621 illus., Hardcover
ISBN: 978-3-319-61275-1